

## **Analysis of Atmospheric Transmission Characteristics in MIR Spectrum of VIIRS**

Yanbiao Sun<sup>1, a</sup>, Xingbang Hu<sup>2, b</sup>, Liqin He<sup>2, c</sup>, Shuaiyang Zhao<sup>2, d</sup>, Lei Yan<sup>1, e\*</sup>

<sup>1</sup>Chinese Academy of Surveying & Mapping, Beijing 100039, China

<sup>2</sup>Institute of Remote Sensing & Geographical Information System, Peking University, Beijing 100871, China

<sup>a</sup>syb51@163.com, <sup>b</sup>xingbang\_hu@163.com, <sup>c</sup>heliqin\_de@126.com, <sup>d</sup>syzhao@pku.edu.cn

<sup>e\*</sup>lyan@pku.edu.cn

**Keywords:** Middle infrared; MODTRAN; Atmospheric transmittance; VIIRS

**Abstract.** The atmospheric transmission is an important parameter affecting the solar radiation and surface thermal radiation. In this paper, MODTRAN radiative transfer model was used to analysis the atmospheric Transmission in middle infrared (MIR) spectrum of VIIRS. We have quantitatively simulated and analyzed the effect of atmospheric profile, aerosol type, visibility, moisture content and observed zenith angle on atmospheric transmittance using the two MIR channels of VIIRS (M12 band and M13-band). The results showed that the transmissivities of the both two middle infrared channels M12 and M13 of VIIRS are influenced by the aerosol type, visibility and observation angle. And the influence of these factors on the M12 channel transmittance are greater impact, in addition, M12 band is strongly influenced by the change of atmospheric profile.

### **Introduction**

Atmospheric transmittance is an important parameter for the radiation of solar and surface, which is also significant in inverting the surface parameters, such as surface temperature, surface reflectivity, etc. When the solar radiation and surface radiation are transport in the atmosphere, they are not only affected by the absorption and scattering of atmospheric molecules such as H<sub>2</sub>O, mixed gases (CO<sub>2</sub>, CO, N<sub>2</sub>O, CH<sub>4</sub>, O<sub>2</sub>)[1], O<sub>3</sub>, N<sub>2</sub>, but also affected by aerosol particles, that will result the radiation attenuation in solar and surface. The medium infrared band is between the visible-near-infrared (VIR) and thermal infrared (IR) bands, so its energy exhibits a unique transition in the transmission process, and its atmospheric transmission characteristics are significantly changed. On the other hand, since the remote sensing load is a band-pass system, the actual energy value measured by the load is greatly affected by the atmospheric transmittance of channels[2]. Therefore, it is necessary to carry out an in-depth analysis on the total atmospheric transmittance and the influence factors of channel transmittance.

Bohui Tang, Zhaoliang Li et al. have analyzed the influence factors of transmittance of the medium-wave infrared channels 22 (3.929-3.989 μm) and 23 (4.020-4.080 μm) of MODIS [3]. But their research were mainly focused on the analysis of aerosol and water vapor content, and did not considered the other influence factors of atmospheric transmittance. In addition, their research were only analyzed the required 22 and 23 channels, ignoring other medium-wave infrared channels. Zhiguo Rong[4], Yonggang Qian[5] have briefly analyzed the characteristics of atmospheric radiation of the medium-wave infrared channel, and did not analyze the transmittance of the medium-wave infrared channel.

In the visible-near-infrared band and the thermal infrared band, there are many literatures on atmospheric transmittance and the study are also mature[6]. However, the atmosphere spectral transmittance and channel transmittance of middle infrared band have not analyzed in detail in the present paper. In this paper, we have use MODTRAN4 radiation correction model[7] to analyze the atmospheric transmittance of the middle wave infrared channels. On this basis, we have

quantitatively simulated and analyzed the effect of atmospheric profile, aerosol type, visibility, moisture content and observed zenith angle on atmospheric transmittance using the two middle infrared channels of VIIRS (M12 band, 3.660-3.840  $\mu\text{m}$ , center wavelength 3.697  $\mu\text{m}$  and M13-band, 3.973-4.128  $\mu\text{m}$ , center wavelength 4.05  $\mu\text{m}$ ).

**The VIIRS Instrument**

The Visible/Infrared Imager Radiometer Suite (VIIRS)[8] is one of the five major Earth observing instruments onboard S-NPP and JPSS. VIIRS signifies a new era of moderate-resolution imaging capabilities following the legacy of AVHRR and Moderate-Resolution Imaging Spectroradiometer (MODIS).

The VIIRS instrument is a whiskbroom scanning radiometer with a field of regard of  $112.6^\circ$  in the cross-track direction. At a nominal altitude of 824 km, the swath width is 3040 km, providing full daily coverage both in the day and night side of the Earth. VIIRS has 22 spectral bands covering the spectrum between 0.412  $\mu\text{m}$  and 12.01  $\mu\text{m}$ , including 16 moderate resolution bands (M-bands) with a spatial resolution of 750 m at nadir, 5 imaging resolution bands (I-bands) – 375 m at nadir, and one panchromatic daynight band (DNB) with a 750 m spatial resolution throughout the scan. The M-bands include 11 reflective solar bands (RSB) and 5 thermal emissive bands (TEB). The I-bands include 3 RSB bands and 2 TEB bands (Tables 1) [9].

Table 1. VIIRS Band Centers, Spatial Resolution, and Gain

Band No.	Driving EDR(s)	Spectral Range ( $\mu\text{m}$ )	Horiz Sample Interval (km) (Track x Scan)		Band Gain	Ltyp or Ttyp (Spec)	Lmax or Tmax	SNR or NE $\Delta$ T (K)	
			Nadir	End of Scan					
Reflective Bands	VIS/NIR	M1 Ocean Color Aerosol	0.402 - 0.422	0.742 x 0.259	1.80 x 1.58	High Low	44.9 155	135 815	352 318
		M2 Ocean Color Aerosol	0.436 - 0.454	0.742 x 0.259	1.80 x 1.58	High Low	40 148	127 887	380 409
		M3 Ocean Color Aerosol	0.478 - 0.498	0.742 x 0.259	1.80 x 1.58	High Low	32 123	107 702	418 414
		M4 Ocean Color Aerosol	0.545 - 0.585	0.742 x 0.259	1.80 x 1.58	High Low	21 90	78 887	382 315
		I1 Imagery EDR	0.800 - 0.880	0.371 x 0.387	0.80 x 0.789	Single	22	718	119
	M5 Ocean Color Aerosol	0.862 - 0.892	0.742 x 0.259	1.80 x 1.58	High Low	10 89	59 851	242 380	
	M6 Atmosph. Correct.	0.739 - 0.754	0.742 x 0.778	1.80 x 1.58	Single	9.8	41	199	
	I2 NDVI	0.848 - 0.885	0.371 x 0.387	0.80 x 0.789	Single	25	349	150	
	M7 Ocean Color Aerosol	0.848 - 0.885	0.742 x 0.259	1.80 x 1.58	High Low	8.4 33.4	29 349	215 340	
	SWMIR	M8 Cloud Particle Size	1.230 - 1.250	0.742 x 0.778	1.80 x 1.58	Single	5.4	185	74
M9 Cirrus/Cloud Cover		1.371 - 1.398	0.742 x 0.778	1.80 x 1.58	Single	8	77.1	83	
I3 Binary Snow Map		1.580 - 1.840	0.371 x 0.387	0.80 x 0.789	Single	7.3	72.5	8	
M10 Snow Fraction		1.580 - 1.840	0.742 x 0.778	1.80 x 1.58	Single	7.3	71.2	342	
M11 Clouds		2.225 - 2.275	0.742 x 0.778	1.80 x 1.58	Single	0.12	31.8	10	
Emissive Bands	LWIR	I4 Imagery Clouds	3.550 - 3.930	0.371 x 0.387	0.80 x 0.789	Single	270	353	2.5
		M12 SST	3.860 - 3.840	0.742 x 0.778	1.80 x 1.58	Single	270	353	0.398
		M13 SST Fires	3.973 - 4.128	0.742 x 0.259	1.80 x 1.58	High Low	300 380	343 834	0.107 0.423
		M14 Cloud Top Properties	8.400 - 8.700	0.742 x 0.778	1.80 x 1.58	Single	270	338	0.091
M15 SST	10.283 - 11.283	0.742 x 0.778	1.80 x 1.58	Single	300	343	0.07		
I5 Cloud Imagery	10.500 - 12.400	0.371 x 0.387	0.80 x 0.789	Single	210	340	1.5		
M16 SST	11.538 - 12.488	0.742 x 0.778	1.80 x 1.58	Single	300	340	0.072		

**Simulation and analysis of VIIRS MIR Channel transmittance**

MODTRAN4(MODERatespectral resolution atmospheric TRANsmittance algorithm and computer model), the newly released version of the U.S. Air Force atmospheric transmission, radiance and flux model is being developed jointly by the Air Force Research Laboratory/Space Vehicles Directorate and Spectral Sciences, Inc. It is expected to provide the accuracy required for analyzing spectral data for both atmospheric and surface characterization.

VIIRS data has 7 TIR channels (3.5~14.5  $\mu\text{m}$ ) among all of its 22 channels. They are channels M12-M16 and channels I4-I5. Therefore, selecting appropriate TIR bands by conditional analysis of atmospheric window is necessary.

Figure 1 shows atmospheric transmissions curve at viewing angle  $45^\circ$  from nadir in mid-latitude summer condition (column water vapor,  $cwv = 2.9 \text{ cm}$ ; surface visibility at  $0.55 \mu\text{m}$ ,  $vis. = 23 \text{ km}$ ). We can see from figure 1 that there are two atmospheric windows in the spectral scope of  $3.5\sim 14.5 \mu\text{m}$ . One is  $8\sim 13 \mu\text{m}$  atmospheric window and the other is  $3.5\sim 4.2 \mu\text{m}$  atmospheric window.

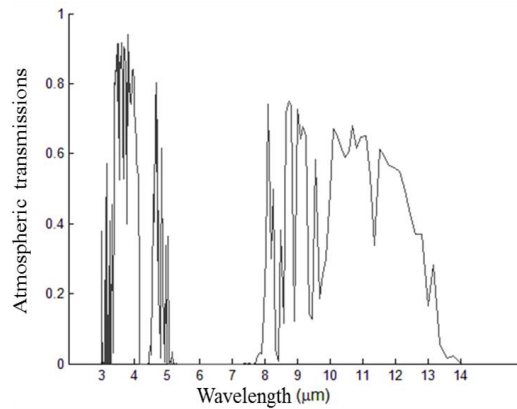


Fig.1 Atmospheric transmissions curve

In this paper, the M12 and M13 channels of VIIRS are taken as an example to analyze the influence factors of the transmittance of medium infrared channel in  $3.5\sim 4.2\mu\text{m}$ . This paper will quantitatively analyze for which atmospheric components or which atmospheric conditions that the transmittance of these two bands will sensitive in the atmospheric correction. First, we use MODTRAN4 to quantitatively analyze the two-channel transmittance on different atmospheric profiles (tropical, mid-latitude summer, mid-latitude winter, sub-polar summer, sub-polar winter, 1976 US standard atmospheric profile), different aerosol models (villages, oceans, cities, troposphere, convective fog, radiation aerosol, etc.), different visibility, different water vapor content and different observation angle. Fig. 2 to Fig. 6 show the transmittance results of M12 and M13 channels of VIIRS that simulated by MODTRAN4 under different influence factors.

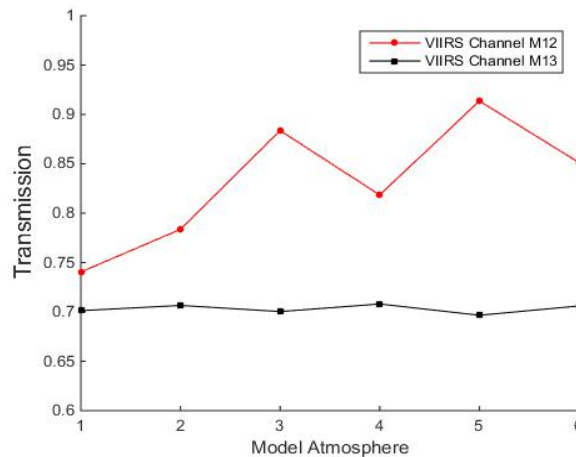


Fig.2 Atmospheric transmissions curve under 6 model atmospheres

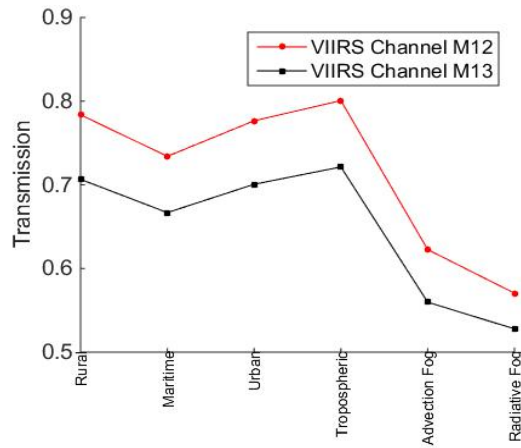


Fig.3 Atmospheric transmissions curve under 6 aerosol models

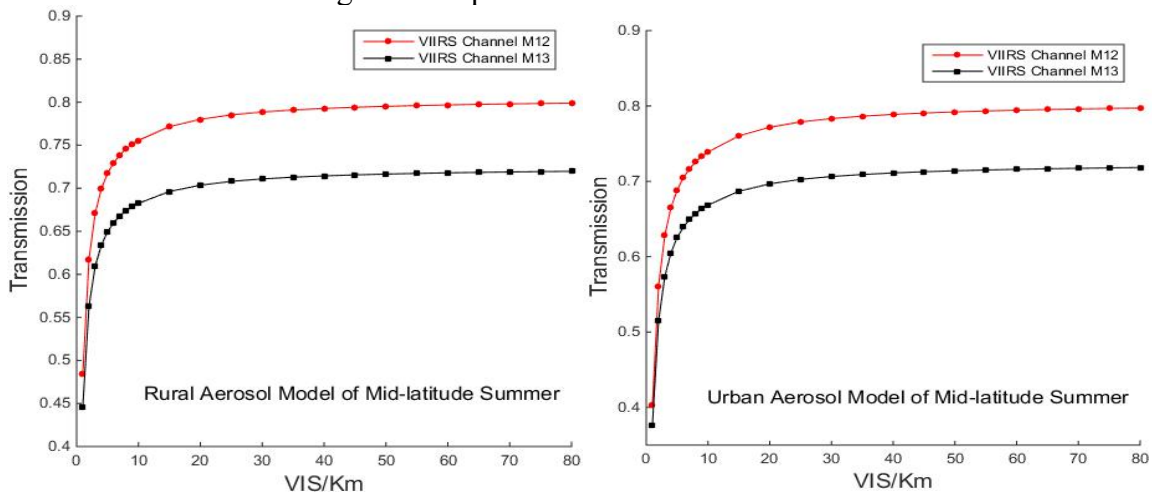


Fig.4 Atmospheric transmissions curve under different visibility in rural aerosol model and urban aerosol model

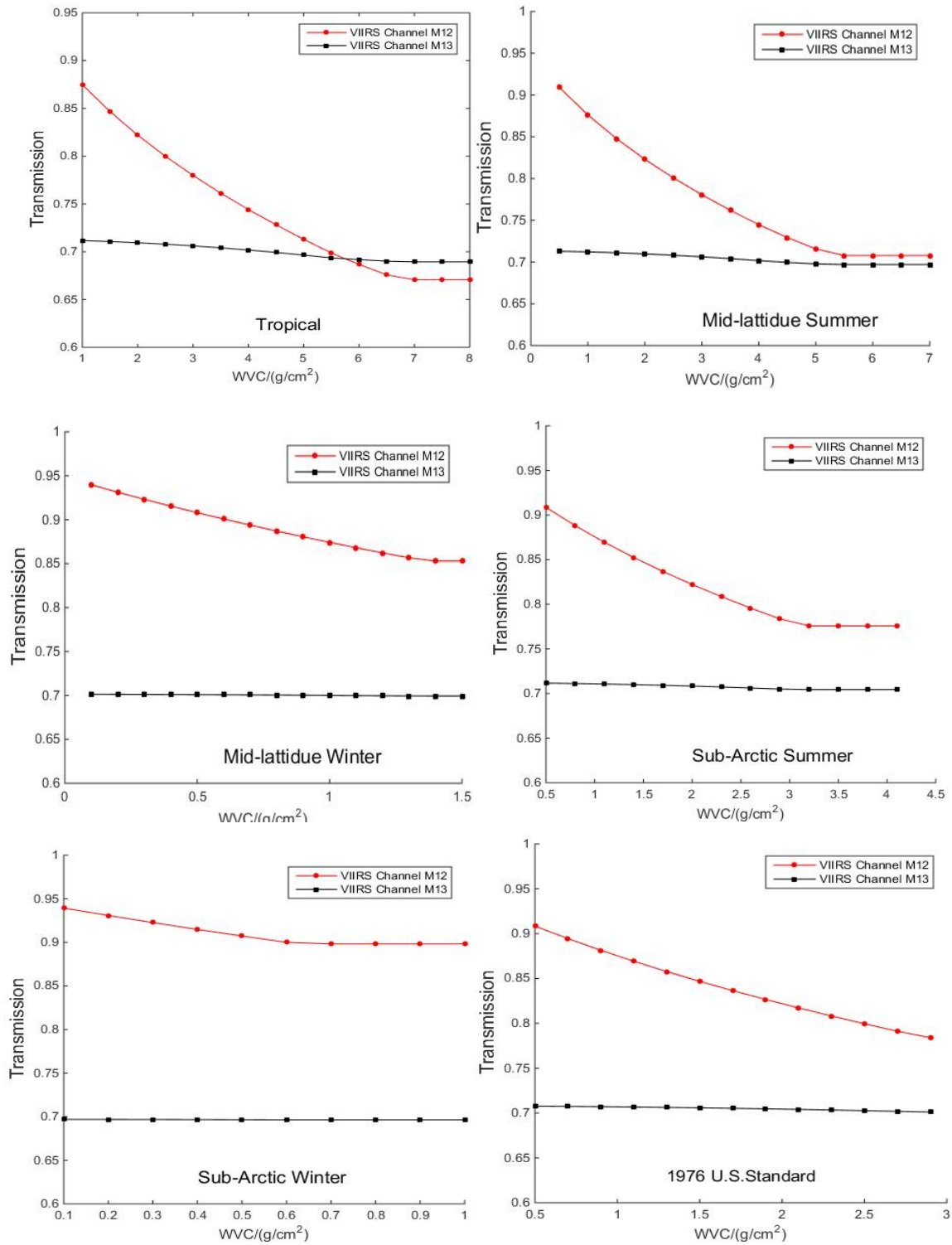


Fig.5 Atmospheric transmissions curve under different WVC in different atmosphere

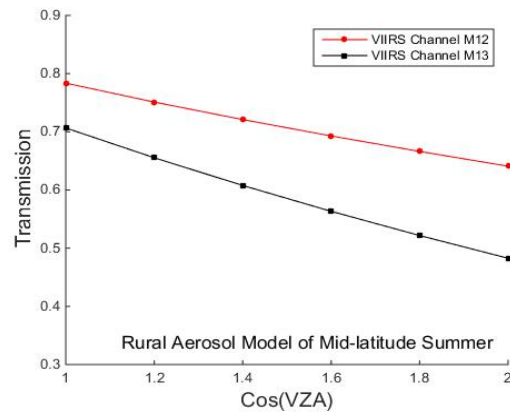


Fig.6 Atmospheric transmissions curve under different view angles

## Conclusions and discussion

From the above simulation curves of channel transmittance, we can find that the transmittances of the both two middle infrared channels M12 and M13 of VIIRS are influenced by the aerosol type, visibility and observation angle. And the influence of these factors on the M12 channel transmittance are greater impact, in addition, M12 band is strongly influenced by the change of atmospheric profile. When the visibility is more than 15Km, the channel transmittance of the two channels in the mid-latitude summer atmospheric profile is less affected by it. The atmospheric transmittance of the M13 channel almost does not change by the water vapor content, but the atmospheric transmittance of the M12 channel affected to a certain extent by it. Therefore, it is necessary to consider the influence of the change of water vapor content when using the M12 channel to invert other parameters (such as surface reflectivity, temperature, etc.). Through the simulation of channel transmittance of the M12 and M13 bands of VIIRS, it is possible to understand the factors that affect the atmospheric transmittance in the middle infrared band. So we can improve the accuracy of atmospheric correction and surface reflectivity inversion results, and on this basis, the inversion algorithm can also do further error analysis.

## Acknowledgements

This work was financially supported by Doctoral Fund of Ministry of Education of China (20130001110046), the National Natural Science Foundation of China (41371492) and the Beijing Natural Foundation (Z151100000915068).

## References

- [1] Psiloglou B E, Santamouris M, Asimakopoulos D N: Renewable energy, 1995, 6(1): 63-70.
- [2] Ruizhong Rao: *Modern Atmospheric Optics* (Science Press, 2012).
- [3] Bohui Tang, Zhaoliang Li, Wu Hua, Tang Rong-Lin: *The research about surface emissivity retrieval in thermal infrared* (Science Press, 2014): 72-75.
- [4] Zhiguo Rong, Yuxiang, Zhang, et al: *Infrared & Laser Engineering*, 2009 38(4):589-593. [5] Yonggang Qian., Enyu Zhao, Caixia Gao, & Ning Wang: *IEEE Journal of Selected Topics in Applied Earth Observations & Remote Sensing*, 2014, 8(99):1208-1216.
- [6] Jinhua Li, Zhibin Wang, Yuanyuan Chen: *Laser & Infrared*, 2013, 43(10):1142-1145.
- [7] Berk, A., Anderson, G. P., Acharya, P. K., Dothe, H., Adlergolden, S. M., & Richtsmeier, S. C., et al.: *The International Society for Optical Engineering*, 1999, 3756, 348-353.
- [8] Arnone, R., Ladner, S., Fargion, G., & Vandermeulen, R: *The International Society for Optical Engineering*, 2013, 8724(3), 363-383.
- [9] Cao C, Xiong J, DeLuccia F, et al.: *User's Guide*, version, 2011, 1.